EGU General Assembly 2020

# What can Hall-MHD simulations tell us about the transition region in the solar wind proton density spectrum?

**V. Montagud-Camps 1,** F. Němec 1, J. Šafránková 1, Z. Němeček 1,
R. Grappin 2, A. Verdini 3,4, A. Pitňa 1

1-Dept. of Surface and Plasma Science, Charles University (Prague)
2-Laboratoire de Physyque des Plasmas (LPP), École Polytechnique (France)
3-Università di Firenze, Dipartimento di Fisica e Astronomia, Firenze, Italy
4-INAF, OAA, Firenze, Italy

EUROPEAN UNION
European Structural and Investment Funds
Operational Programme Research,
Development and Education

MINISTRY OF EDUCATION,
YOUTH AND SPORTS

# Introduction

The spectrum of density fluctuations in the solar wind shares features similar to those of kinetic and magnetic fluctuations. Namely, a range of frequencies above the proton gyro-frequency where the spectrum scales as f^(-3/2) or f^(-5/3) and a sub-proton range where the spectral index can vary between -2 and -4.

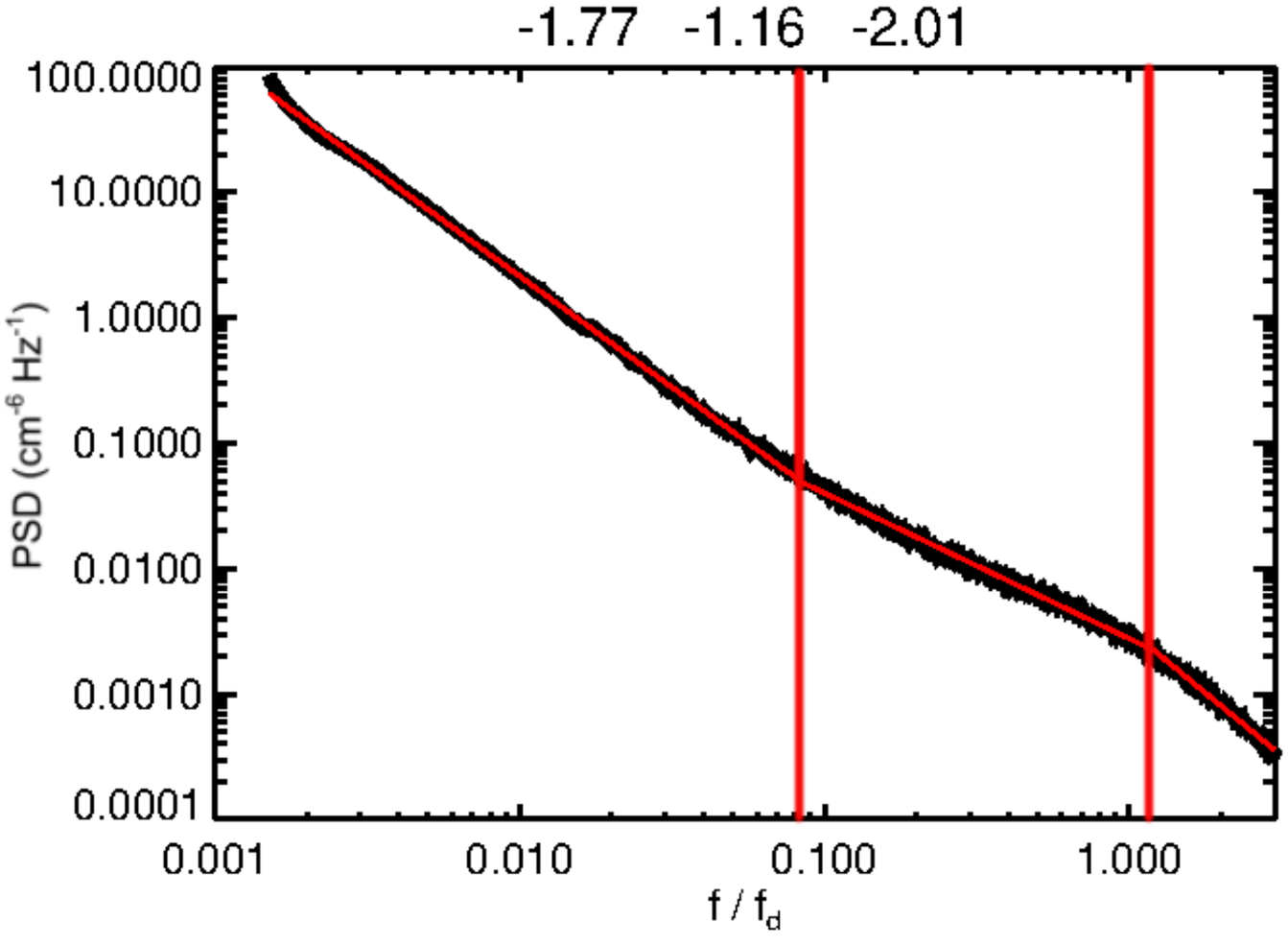


*Fig.: Proton density spectrum at 1 au obtained from BMSW instrument on-board of Spektr-R satellite. Index of the three fitted power laws are shown above the figure. Data selection will be specified during the presentation.*

However, unlike kinetic and magnetic spectra, a one-decade flattening of the density spectrum is observed above the proton gyro-frequency. At this **transition region**, the density spectrum typically scales as 1/f, although positive slopes have also been reported.

# Introduction

The formation of the transition region is still an open question and, as such, several theories have arisen to explain its formation over the years (e.g. Neugebauer 1978, Harmon and Coles 2005). Recent observations at 1au (Chen et al. 2013, Šafránková et al. 2015, Treumann et al. 2019) have shown good agreement consistent with the model presented in Chandran et al. 2009 (CH09).

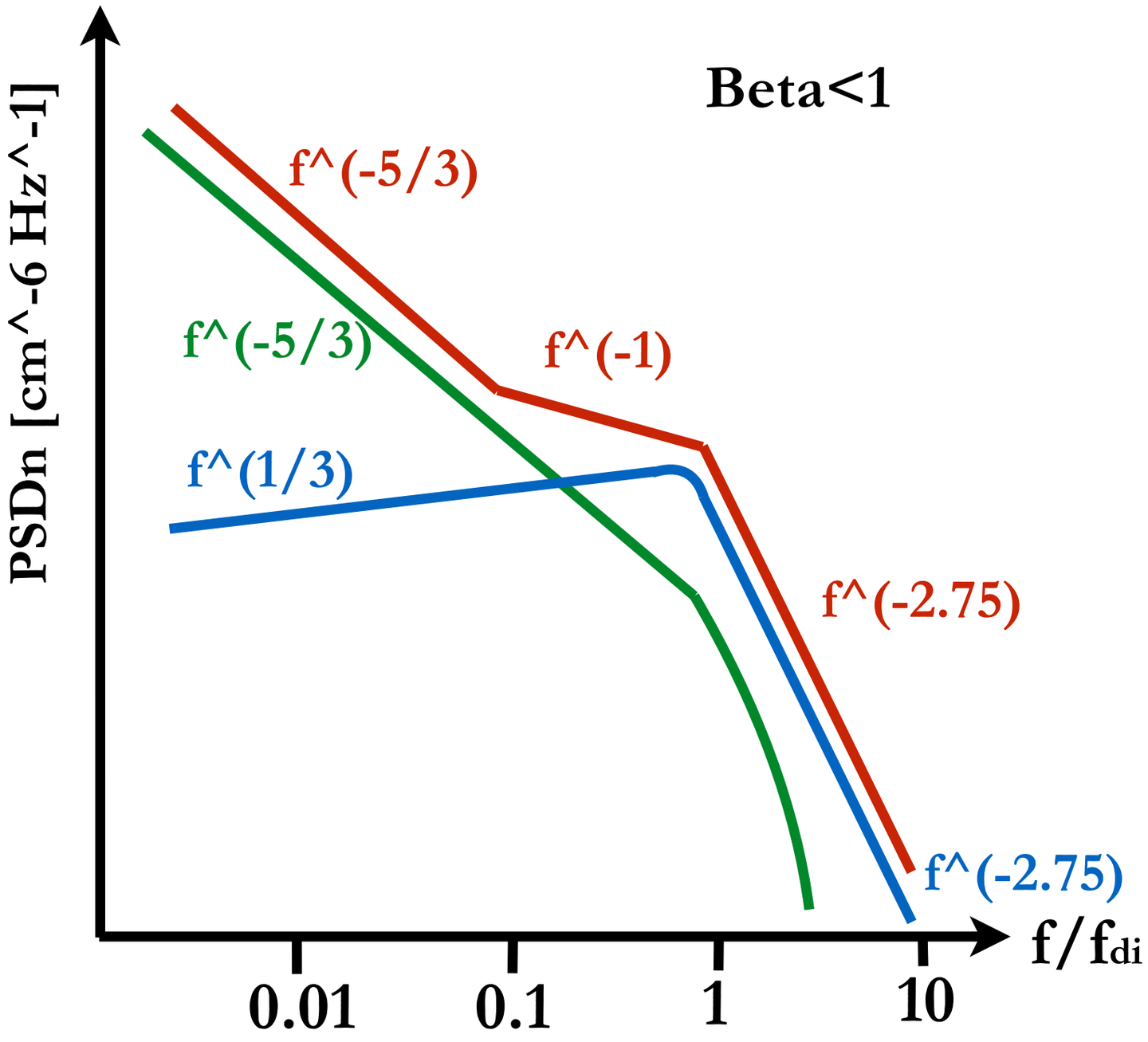


In that paper, Chandran et al. proposed that the **observed spectrum of density fluctuations** would be the superposition of a **"passive spectrum"** and an **"active spectrum"**, generated by non-linear interactions of Kinetic Alfvén waves.
The superposition of both spectra would then give rise to the observed transition region.

# Motivation and objectives

Without additional knowledge about the contributions of the passive and active components, CH09 model cannot give a prediction of the spectral index in the transition region. However, one can expect that for plasma with low enough beta, the KAW contribution would rise, allowing to see a transition region with a 1/3 slope.

Such a slope has been observed at 1 au (Treumann et al. 2019). Conversely, in coronal holes, where plasma beta can be two orders of magnitude lower than at 1 au, radio scintillation measurements of density fluctuations show a flattening at the transition frequencies close to f^(-1.38) (Harmon and Coles 1989 and 2005).

Our objectives are, on the one hand, to test with numerical simulations if a flattened region in the density spectrum can arise from non-linear interaction of high-frequency plasma waves. On the other hand, based on our simulation results and observations at 1au, we propose an explanation for the steep slope that the transition region of the density spectrum presents in coronal holes.

# Numerical setup

We discuss here the results of a compressible MHD and a compressible Hall-MHD simulations with no forcing, zero initial cross-helicity and residual energy, initial isotropic spectra of magnetic and kinetic fluctuations with random phases, excited down to $k_{cut}=16$ with an initial scaling of k^(-2). No density fluctuations are initially excited.
We take periodic boundary conditions for our numerical domain, which is a 3D cube with a uniform grid. The size of the box remains constant over time (no plasma expansion nor shearing effects). Both simulations run for 7.5 non-linear times $t_{NL,0}= 1/(u_0 k_{max})$.
The proton inertial length, $d_i$ is expressed as a fraction of the box edge, $L_{max}$. Notice that the wavenumber corresponding to $d_i$ in the Hall-MHD simulation will be **$k d_i=10$**.

| Run | Resolution | $B_0$ | Beta | $db/B_0$ | Initial slope | $d_i$ [$L_{max}$] |
|---|---|---|---|---|---|---|
| **MHD** | 256^3 | (5,0,0) | 0,2 | 0,2 | k^(-2) | 0 |
| **H-MHD** | 256^3 | (5,0,0) | 0,2 | 0,2 | k^(-2) | 0,1 |

# Reduced density spectrum ($k_{par}$)

We have divided the simulations into five intervals with the same duration (bottom legend in figure below). We have then time-averaged the parallel density spectrum within each of the five intervals. In the image below we show the resulting five mean density spectra compensated by k^(3/2), with the upper spectrum corresponding to the first times of the simulation.

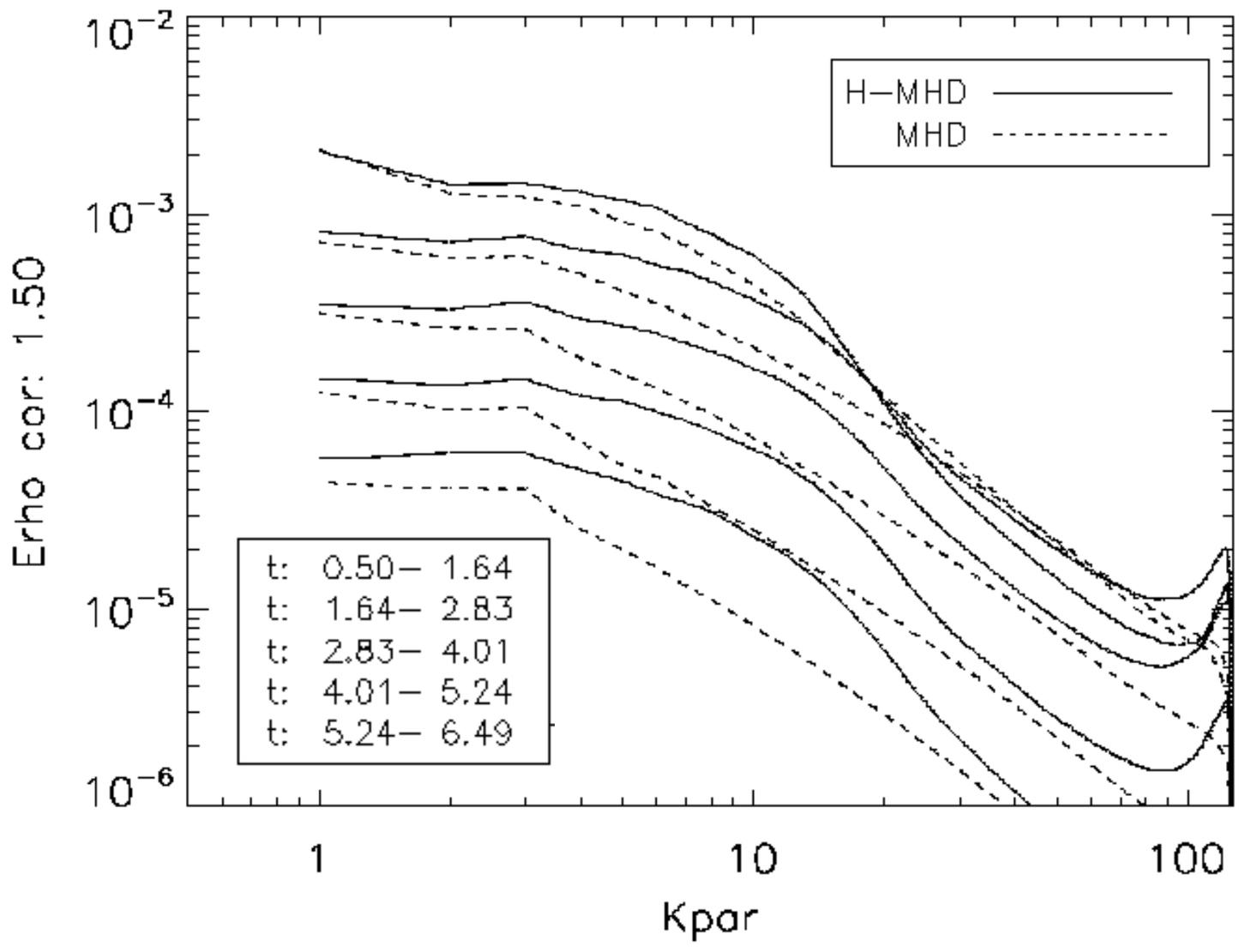

# Reduced density spectrum ($k_{perp}$)

Same caption as in the previous slide, but in this case, the density spectra have been computed along kz (perpendicular to B0) and compensated by k^1.
The Hall-MHD simulation develops a k^(-1) range during the last two intervals of the simulation.
As it will be shown in the next slide, such scaling anisotropy at the transition region is also present in solar wind observations.

**En(kz)kz^(1)**

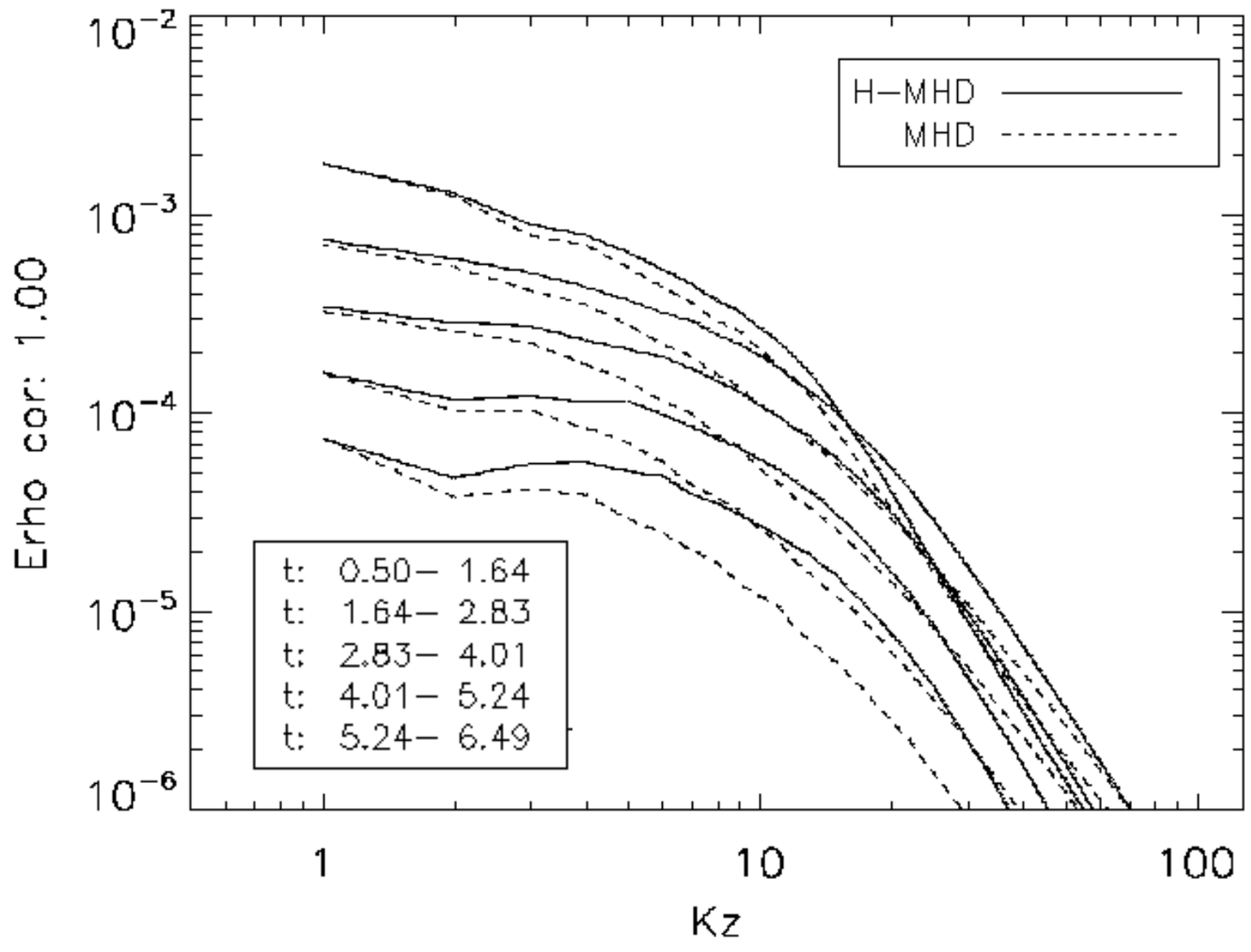

# In-situ observations at 1au

From the proton density fluctuations measured at 1 au by BMSW instrument on board of Spektr-R satellite, we have selected 20.188 time intervals with a maximum duration of 20 min. and 31 ms resolution for solar winds with plasma beta lower than 0.1. Intervals have been taken in the time range between September the 3rd of 2011 and to November 28th 2018.

Since magnetic fluctuations cannot be measured on board of Spektr-R, we have propagated the mean magnetic field measured at Wind with MFI during satellite alignments, following the procedure explained in Pitňa et al. 2019. We have then gathered the intervals in two groups depending on the angle of the mean magnetic field with respect to solar wind bulk velocity: **for angles smaller than 30° or larger than 150° (left panel) and angles between 60° and 120° (right panel)**.

We have fitted the resulting spectra with three power laws, whose index are indicated above the figures. We remark a scale anisotropy for the transition region, where the flattening is less pronounced for low cone angles.

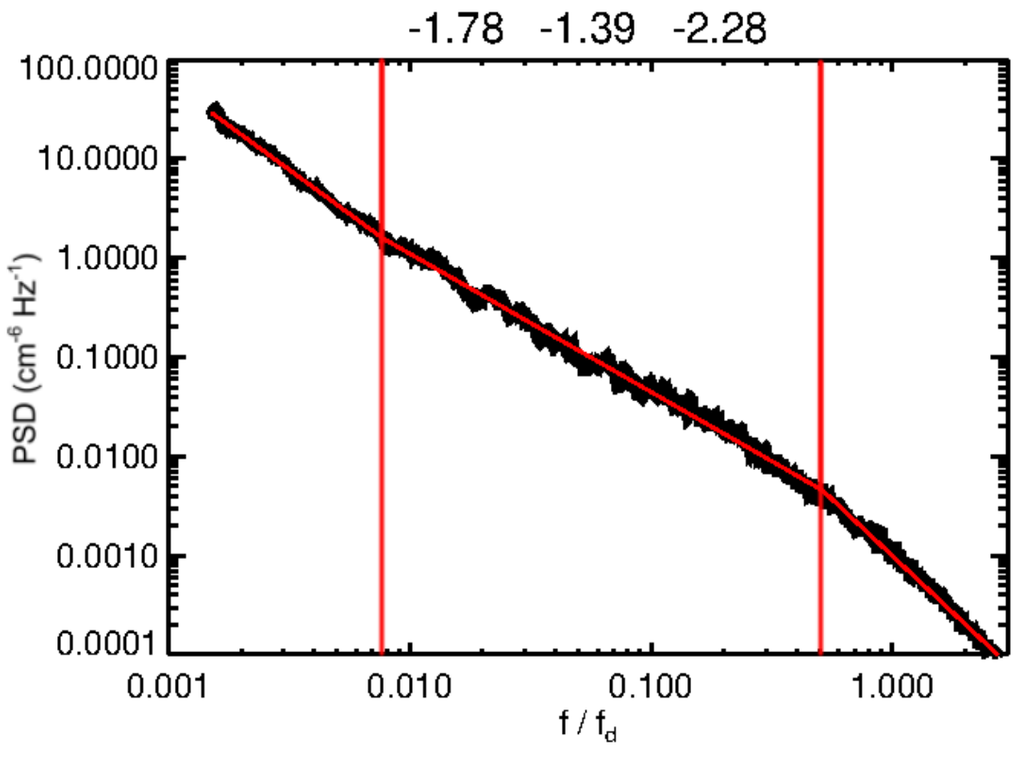


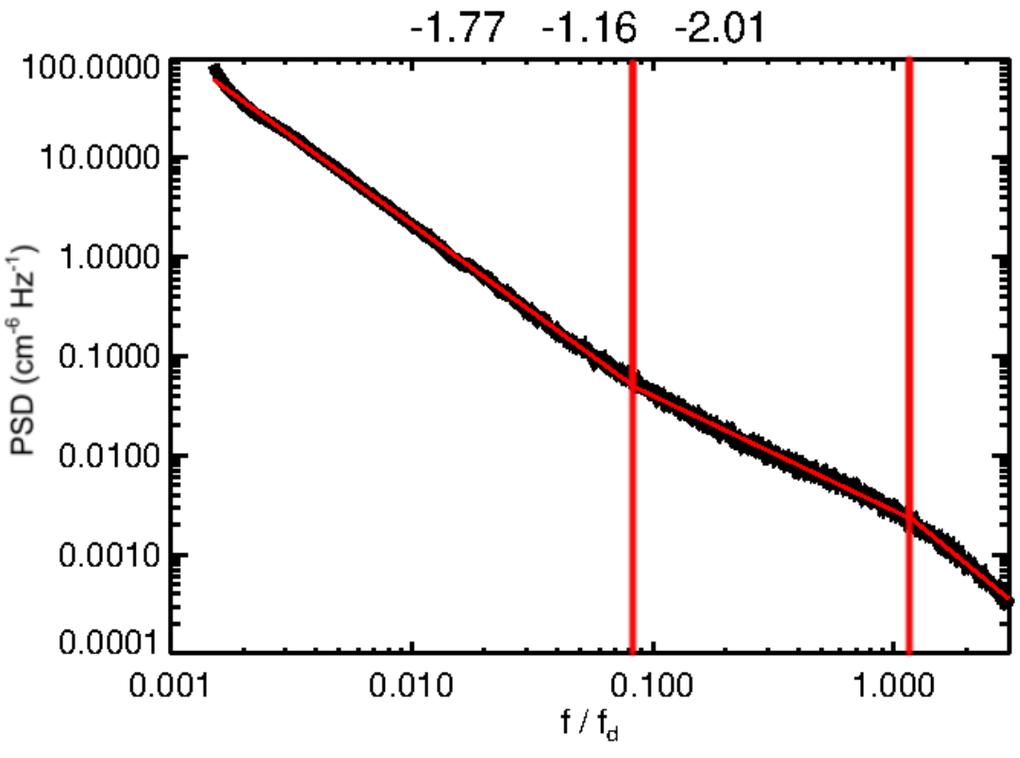

# Spatio-temporal spectrum

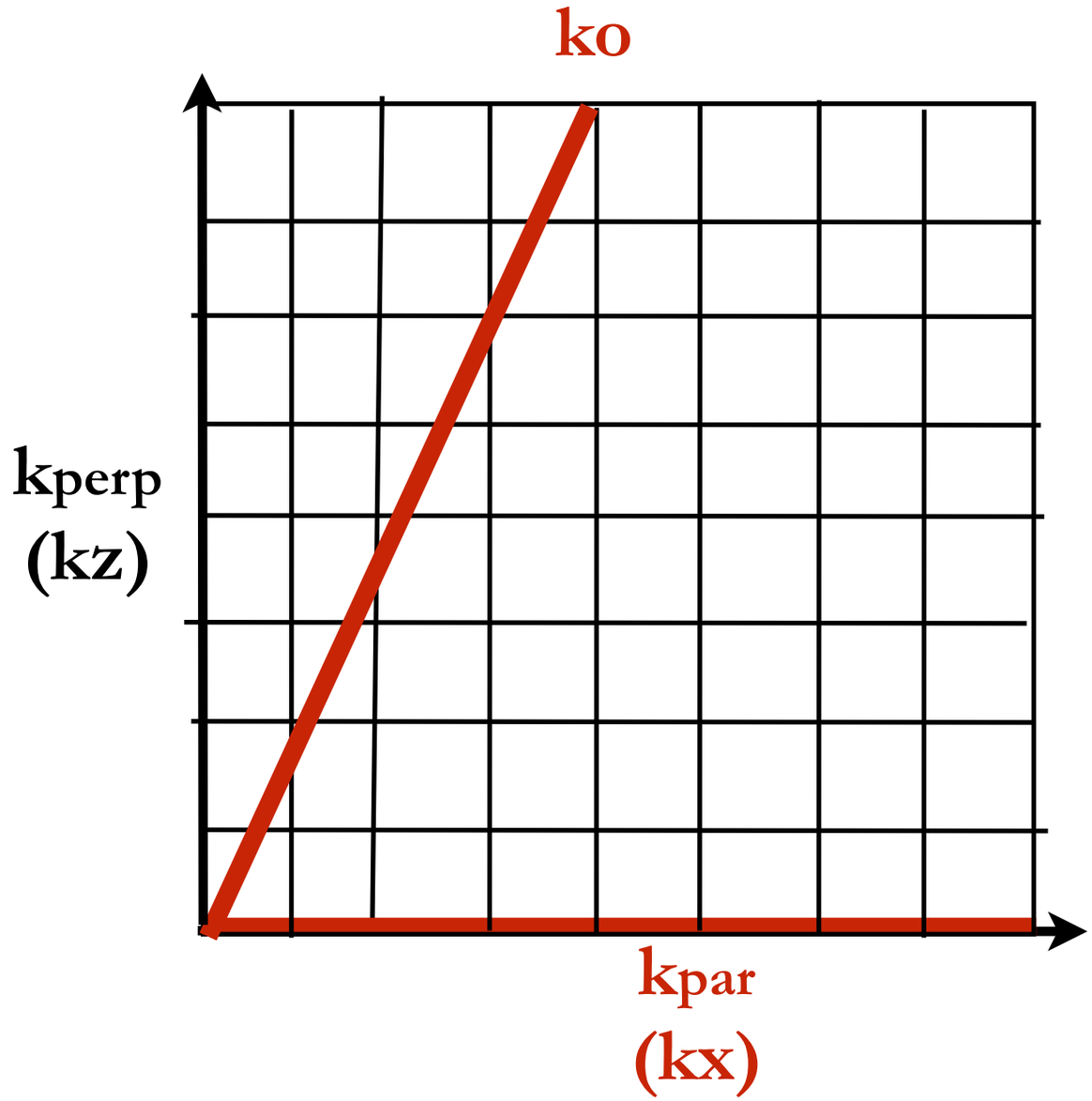


Similarly to Andrés et al. 2017, we show the spatio-temporal spectrum of density fluctuations in order to identify plasma waves in our simulations.
First, we have taken 2D cuts of density fluctuations in Fourier space, dn(kx,ky=0,kz,t). Then, 1D cuts are taken in the directions marked with red lines in the left figure: kx (parallel direction to B0), and **ko** (oblique direction such as $k_{oz,max}/k_{ox,max}=2$, about **63.4° with respect to $B_0$**).
Fluctuations are interpolated to obtain dn(ko,t) along ko with constant separation between wavenumbers.
The temporal signal for each wavenumber is also interpolated to obtain constant cadence. We then have applied a tapered cosine window with shape parameter 0.5 between $0.5t_{NL,0}$ and $7.5t_{NL,0}$ to every time signal in order to force periodicity. We have applied a Fourier transformation to the time signal for each wavenumber. Finally, the spatio-temporal spectrum is obtained as:
Sn(w,k)=(1/2)|dn(w,k)|^2

# 4-Dispersion relations

Here, we present the dispersion relations that will be shown in the spatio-temporal specta. For the sake of clarity, we have not included the entropy (w=0 ) nor the acoustic modes (w=$c_s$k).

Alfvén Waves (**AW**) $\omega = \pm v_a k \cos\theta_{kB}$

Fast Magnetosonic Waves (**F-MS**) $\omega = \pm k\sqrt{\frac{1}{2}(c_s^2 + v_a^2 + \sqrt{(c_s^2+v_a^2)^2 - 4c_s^2 v_a^2 \cos\theta_{kB}})}$

Slow Magnetosonic Waves (**S-MS**) $\omega = \pm k\sqrt{\frac{1}{2}(c_s^2 + v_a^2 - \sqrt{(c_s^2+v_a^2)^2 - 4c_s^2 v_a^2 \cos\theta_{kB}})}$

Whistler Waves (**Ws**) $\omega = \pm v_a d_i \cos\theta_{kB} k^2$

Ion-Cyclotron Waves (**IC**) $\omega = \pm \frac{k\cos\theta_{kB}}{k}\frac{v_a}{d_i}$

Kinetic Alfvén Waves (**KAW**) $\omega = \pm(v_a k \cos\theta_{kB})\sqrt{1 + (d_i k \sin\theta_{kB})^2(\gamma\beta/4)}$

# Spatio-temporal density spectra

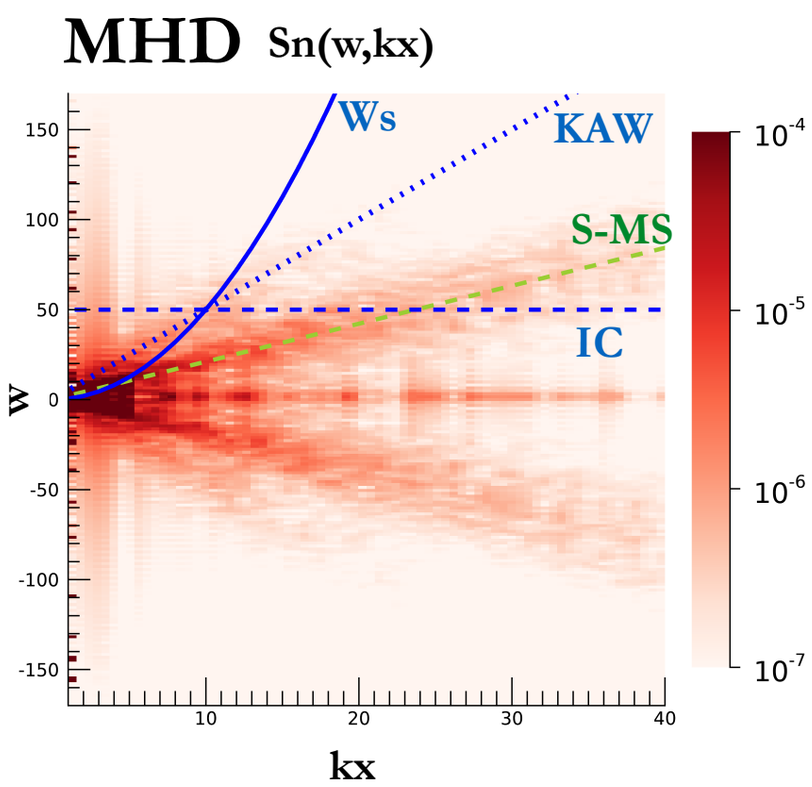


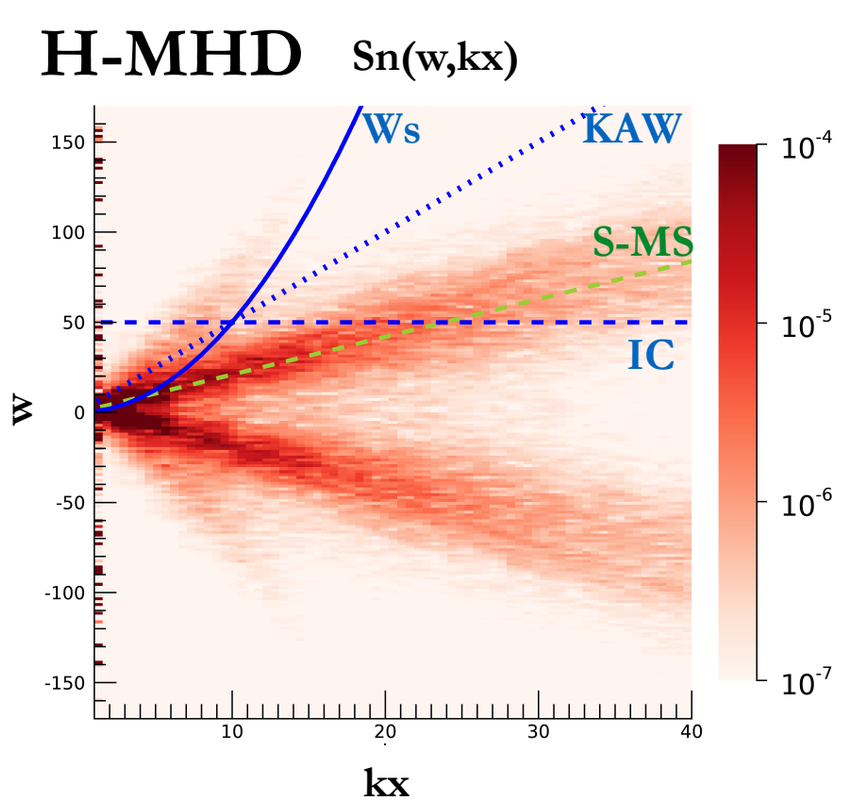


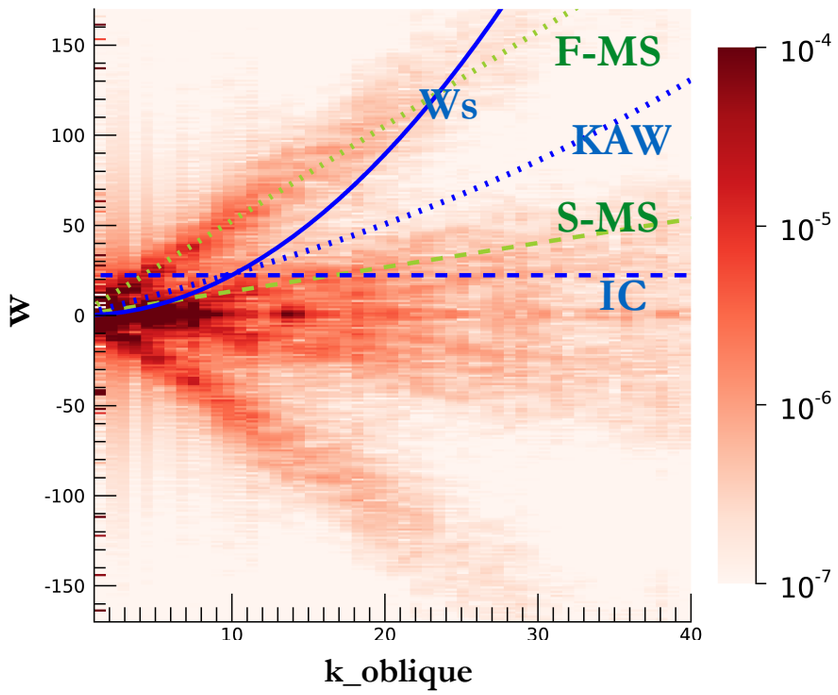


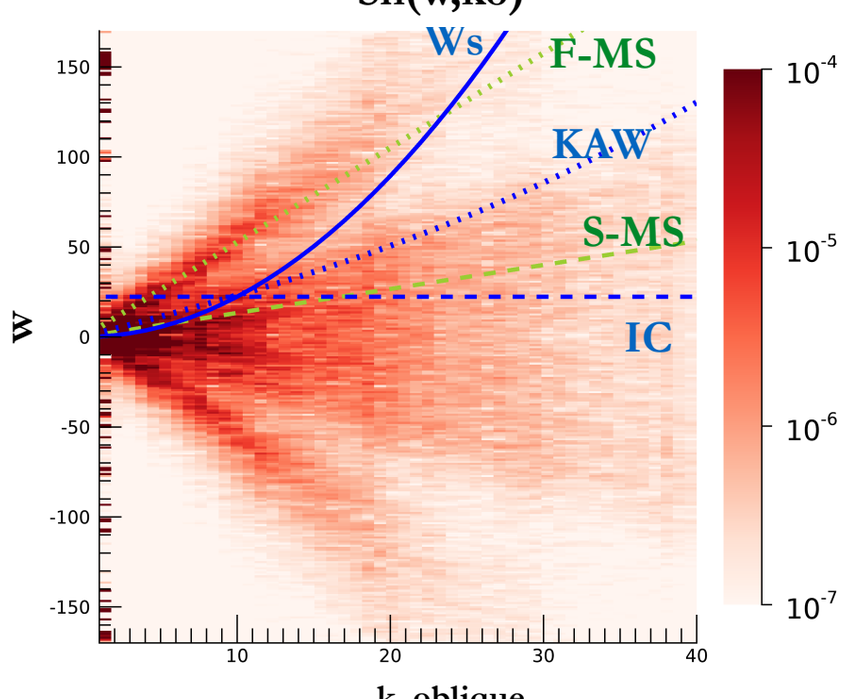


Along the parallel direction, the main contribution comes from the slow magnetosonic modes for MHD and H-MHD simulations. Minor contributions come from the entropy mode (w=0) in the MHD, while for the H-MHD simulation energy accumulates following the whistler branch.

Along the oblique direction, energy accumulates along the fast and slow magnetosonic modes. However, for the H-MHD simulation, energy spreads up to the KAW branch.

# Summary and Conclusions.

-Only the Hall-MHD simulation has managed to reproduce a clear and steady transition region for the reduced density spectrum. Thus, our simulations support that the flattening observed in the density spectrum can be caused by non-linear interaction of high frequency waves.

-Hall-MHD simulations and satellite observations, show that the slope in the transition region becomes steeper when the reduced spectrum is measured along magnetic field aligned directions. We propose that the steep slopes observed in coronal holes are a consequence of this scaling anisotropy and the magnetic field being more aligned with the line-of-sight of the measurements. We expect that PSP and SO measurements will allow to test this idea.

-The spatio-temporal spectra of density fluctuations has shown us that 1)the entropy mode does not contribute to the energy of density fluctuations in the Hall-MHD simulation; 2) in MHD and H-MHD simulations there is an important contribution of fast and slow magnetosonic modes; 3) there is a contribution of KAW to density fluctuations that is observed along oblique directions.

-Finally, we remark that other models of the density spectrum such as NI-MHD (Matthaeus et al. 93) can provide an alternative explanation for the large scale density spectrum and for the formation of the transition region without necessarily rely on KAW turbulence.

# References


Andrés N, Clark di Leoni P, Mininni PD, Dmitruk P, Sahraoui F, Matthaeus WH (2017) Interplay between Alfvén and magnetosonic waves in compressible magnetohydrodynamics turbulence. Physics of Plasmas 24(10):102314, DOI 10.1063/1.4997990

W. A. Coles, and J. K. Harmon, Astrophys. J. 337, 1023(1989)

Chandran BDG, Quataert E, Howes GG, Xia Q,Pongkitiwanichakul P (2009) Constraining low-frequency alfvénic turbulence in the solar wind using density-fluctuation measurements, The Astrophysical Journal 707(2):1668–1675, DOI 10.1088/0004-637x/707/2/1668

Chen CHK, Howes GG, Bonnell JW, Mozer FS, Klein KG, Bale SD (2013) Kinetic scale density fluctuations in the solar wind. AIP Conference Proceedings 1539(1):143–146, DOI 10.1063/1.4811008

J. K. Harmon, and W. A. Coles, J. Geophys. Res. 110,3101 (2005)

Matthaeus WH, Klein LW, Ghosh S, Brown MR (1991) Nearly incompressible magnetohydrodynamics, pseudosound, and solar wind fluctuations. Journal of Geophysical Research:Space Physics 96(A4):5421–5435, DOI 10.1029/90JA02609

M. Neugebauer, C. S. Wu, and J. D. Huba, J. Geophys.Res. 83, 1027 (1978)

Pitňa A, Šafránková J, Němeček Z, Franci L,Pi G, Camps VM (2019) Characteristics of solar wind fluctuations at and below ion scales. Astrophysical Journal 879(2):82, DOI 10.3847/1538-4357/ab22b8

Treumann RA, Baumjohann W, Narita Y (2019)On the ion-inertial-range density-power spectra in solar wind turbulence. Annales Geophysicae 37(2):183–199, DOI 10.5194/angeo-37-183-2019

Šafránková J, Němeček Z, Němec F, Přech L,Pitňa A, Chen CHK, Zastenker GN (2015) Solar wind density spectra around the ion spectral break. The Astrophysical Journal 803(2):107,DOI 10.1088/0004-637x/803/2/107

# Acknowledgements

This research was supported by OP RDE project No. CZ.02.2.69/0.0/0.0/16_027/0008495, International Mobility of Researchers at Charles University

This work was supported by The Ministry of Education, Youth and Sports from the Large Infrastructures for Research, Experimental Development and Innovations project "IT4Innovations National Supercomputing Center – LM2015070"

Access to CESNET storage facilities provided under the programme "Projects of Large Research, Development, and Innovations Infrastructures“ (CESNET LM2018140), is acknowledged.

# Appendix A: 1D magnetic spectra

**Eb(kx)kx^(3/2)**

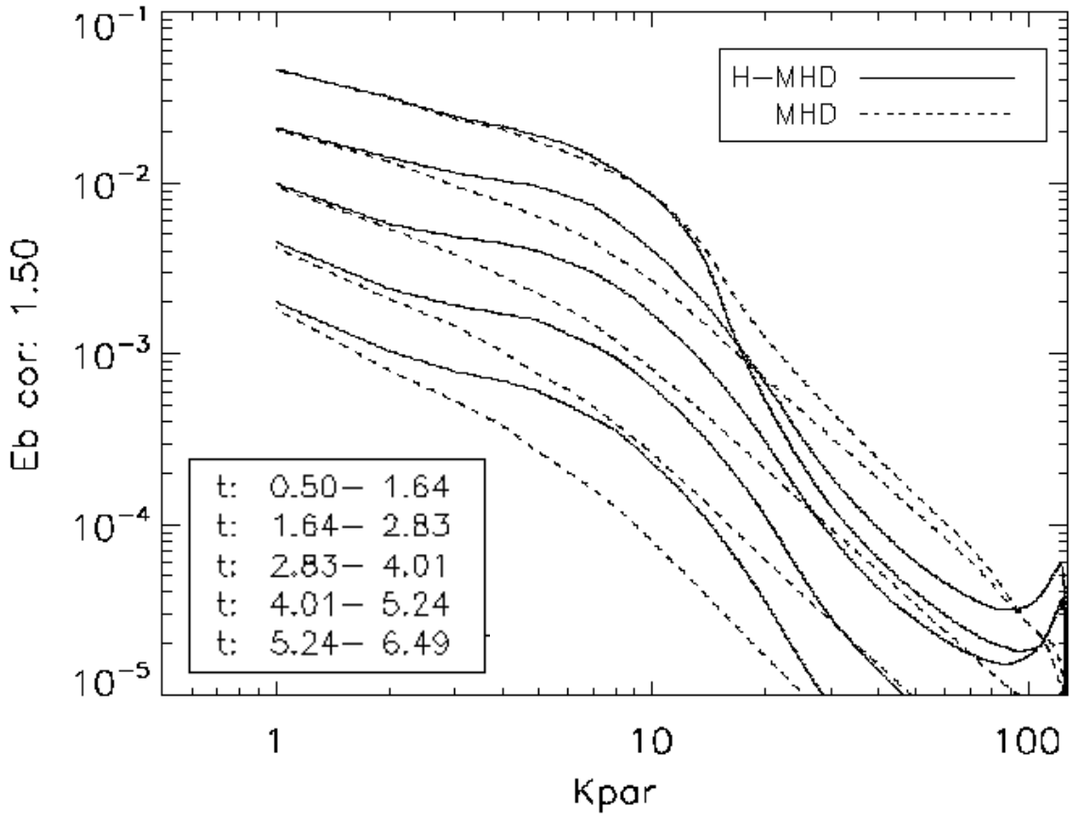


**Eb(kz)kz^(3/2)**

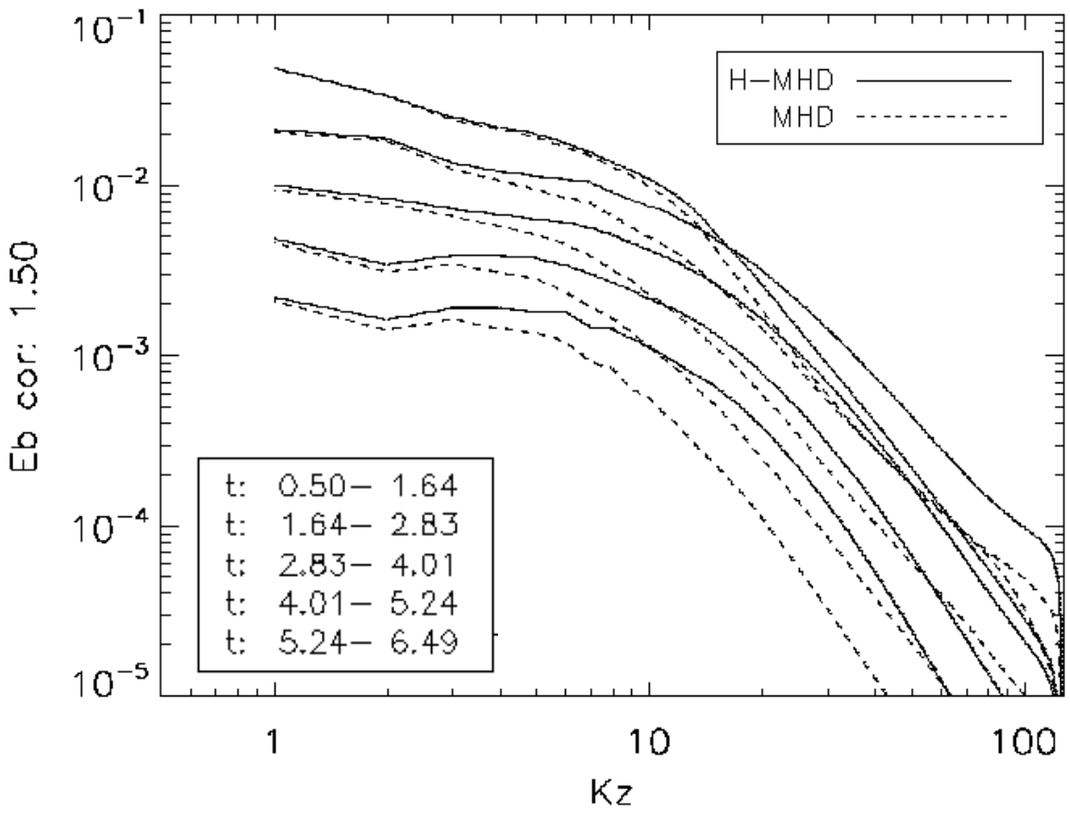

# Appendix B: 1D kinetic spectra

**Eu(kx)kx^(3/2)**

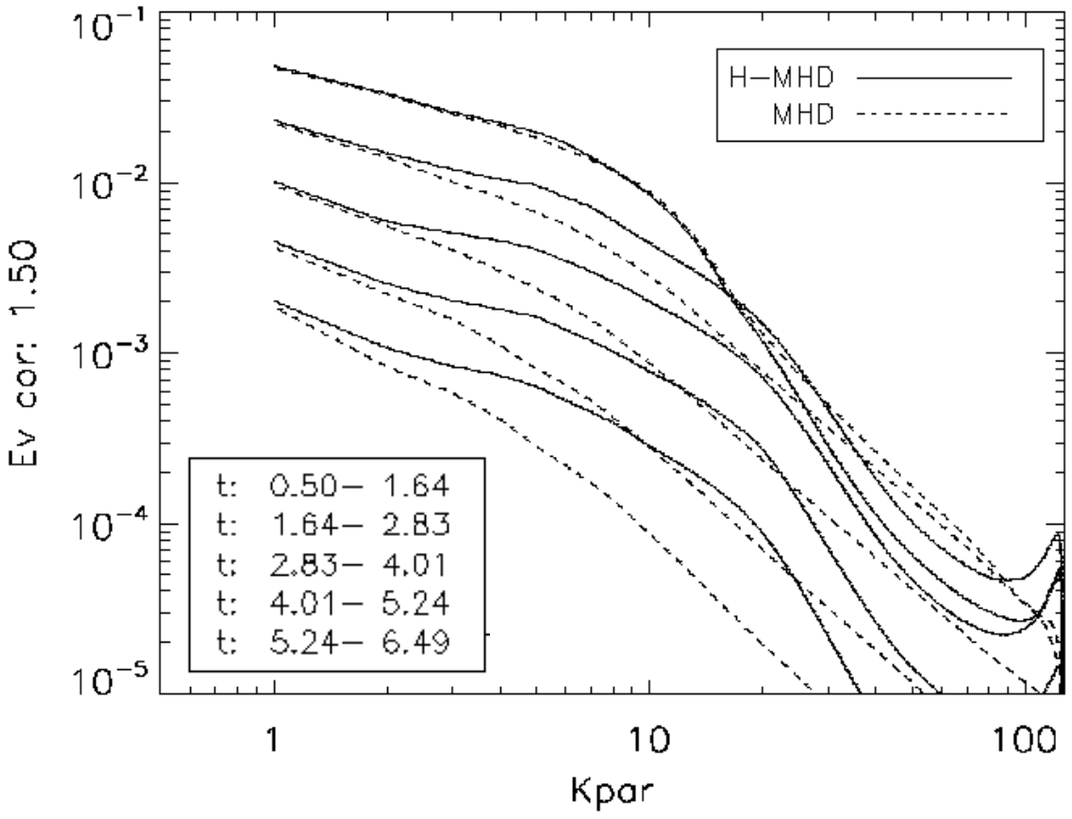


**Eu(kz)kz^(3/2)**

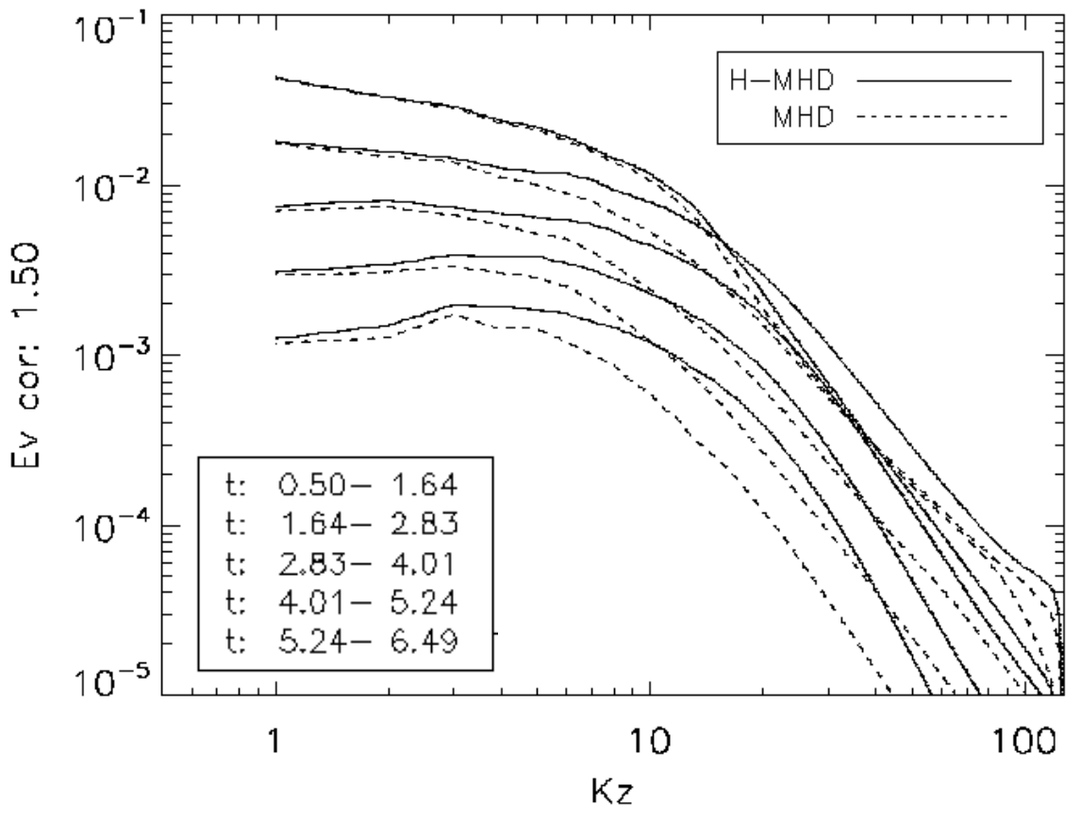

# Appendix C: Spatio-temporal density spectra at low wavenumbers

Here, we show the spatio-temporal spectrum of density fluctuations for the MHD and H-MHD simulation for k_oblique<10. Temporal signal has been taken between $4t_{NL,0}$ and $7.5t_{NL,0}$. This selection roughly corresponds to the times and region in Fourier space that display the k^(-1) power law in the reduced density spectrum along kz.
We consider that the information extracted from this selection is in line with the results shown in previous slides and, due to the limited resolution, no new information can be obtained from the images below.
We note that the odd energy contributions observed along k=1 are consequence of the periodization procedure applied to time signals.

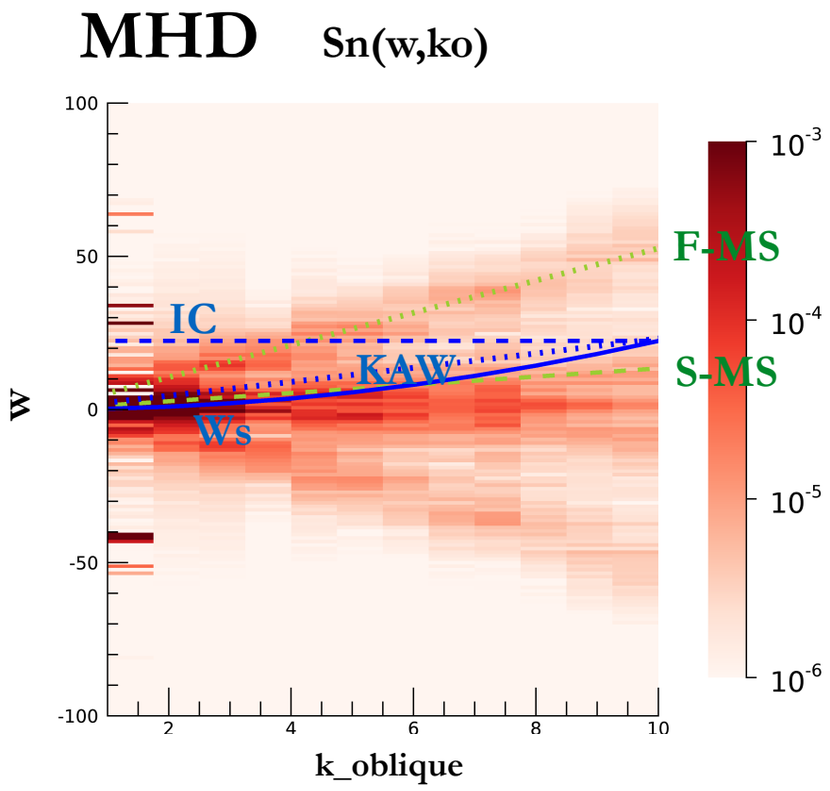


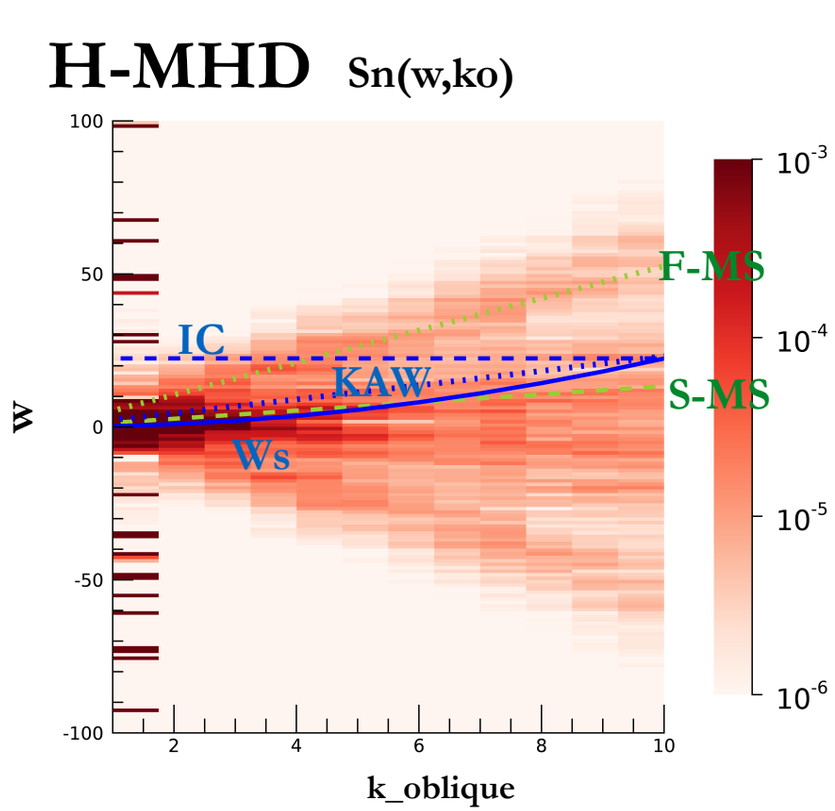

# Appendix D: Spatio-temporal Bz spectra